Chemical Geology 460 (2017) 84–92

Contents lists available at ScienceDirect

Chemical Geology

journal homepage: www.elsevier.com/locate/chemgeo

Molybdenum isotope fractionation and speciation in a euxinic lake—Testing ways to discern isotope fractionation processes in a sulfidic setting

Tais W. Dahl[a,*], Stefanie B. Wirth[b]

[a] Nordic Center for Earth Evolution, Natural History Museum of Denmark, University of Copenhagen, Øster Voldgade 5-7, DK-1350 Copenhagen K, Denmark
[b] Centre for Hydrogeology and Geothermics (CHYN), University of Neuchâtel, Neuchâtel, Switzerland

ARTICLE INFO

Keywords:
Molybdenum
δ^{98}Mo
Stable isotope fractionation
Euxinic environments
Mo speciation
Mo-XANES
Lake Cadagno

ABSTRACT

The molybdenum (Mo) isotope composition in euxinic shales has been used as a proxy for the global distribution of anoxic conditions in ancient oceans, and since more recently also as a proxy for sulfide concentrations in depositional environments. However, there is currently no way to distinguish isotope fractionation at low bottom water sulfide concentrations in 'local' basins from 'global' secular isotope variations associated with changing seawater composition. This uncertainty is challenging the use of Mo isotopes for paleoceanographic reconstructions.

To explore this further, we present new data from sediments deposited over the past ~9800 years in one of the best studied euxinic localities in the world: Lake Cadagno in Switzerland. The sample set allows us to test ways to discern isotope fractionation processes at play in a highly restricted euxinic basin.

Most of our drill core samples (n = 18) show high δ^{98}Mo values similar to previously studied shallow sediments, indicative of quantitative Mo removal from the water column (Dahl et al. 2010a). However, a few samples (n = 3) deposited between about 1200 and 3400 years ago carry low δ^{98}Mo values and have been isotopically fractionated in the lake. Sedimentological and geochemical characterizations show that these δ^{98}Mo-fractionated sediments formed during times of frequent injection of O_2- and sediment-rich river water into the deep sulfidic water column. A positive correlation between δ^{98}Mo and sedimentary Mo contents suggests that isotope fractionation occurred during times of non-quantitative Mo removal, although Mn-oxide cycling at the chemocline might also contribute a subordinate proportion of (^{98}Mo-depleted) molybdenum into the sulfidic zone. Sedimentary Mo/U enrichments relative to oxic lake water further supports the hypothesis that a particulate Mo shuttle was most efficient during times of quantitative Mo removal. Therefore, periods with inefficient Mo capture are ascribed to incomplete conversion of molybdate to particle reactive Mo species when bottom water H_2S levels were low or less stable than today.

Using XAFS spectroscopy, we found that the two distinct Mo compounds predominating in the sediments (Mo^{IV}-S and Mo^{VI}-OS) are not diagnostic for isotope fractionation that has occurred in Lake Cadagno. Instead, we infer that δ^{98}Mo-fractionated products (forming via a low-sulfide Mo pathway) can be subsequently altered with little or no isotopic imprint during remobilization and re-precipitation (e.g., at higher sulfide levels in the sediments) as well as during post-depositional oxidation.

Future work could investigate local δ^{98}Mo-fractionation processes expressed in other euxinic settings and explore other sedimentary metrics to constrain the steps involved in the euxinic burial pathway(s). One tantalizing prospect of this is to distinguish between local bottomwater sulfide levels and variations in the fraction of global seafloor anoxia from the Mo isotope composition in ancient euxinic mudrocks.

1. Introduction

1.1. The δ^{98}Mo record and ancient ocean chemistry

The molybdenum isotope composition of ancient black shales holds important clues to the evolution of the oxygenation state of Earth's oceans (Arnold et al., 2004; Barling et al., 2001; Chen et al., 2015; Dahl et al., 2010b; Dickson et al., 2014; Duan et al., 2010; Gordon et al., 2009; Kendall et al., 2009, 2011, 2015; Pearce et al., 2008; Siebert et al., 2003; Wille et al., 2007). Yet, not all black shales display the isotope composition of contemporaneous overlying seawater (e.g., Baldwin et al., 2013; Dahl et al., 2011, 2010b; Gordon et al., 2009;

* Corresponding author.
E-mail address: tais.dahl@snm.ku.dk (T.W. Dahl).

http://dx.doi.org/10.1016/j.chemgeo.2017.04.018
Received 23 January 2017; Received in revised form 11 April 2017; Accepted 16 April 2017
Available online 18 April 2017

Herrmann et al., 2012), because isotope fractionation is expressed between the sediments and seawater whenever Mo removal from the water column is incomplete.

At least two processes can induce a net Mo isotopic offset between Mo in surface waters and euxinic sediments. First, Mo adsorbing onto Mn-oxides in oxic seawater induce strong isotope fractionation (− 3‰) that might be transported across the chemocline into deeper anoxic bottomwaters and sediments (Neubert et al., 2008; Noordmann et al., 2015; Reitz et al., 2007). Secondly, Mo isotope fractionation occurs during sulfidation of molybdate to thiomolybdate species. This process is associated with isotope fractionation (Tossell, 2005; Kerl et al., 2017) that may be preserved in sediments when bottomwater hydrogen sulfide concentrations are low (e.g., H_2S < 11 μM) and/or there is not enough time available for Mo to react with sulfide and convert to reactive Mo compounds (Dahl et al., 2010a; Nägler et al., 2011; Neubert et al., 2008). This sensitivity towards hydrogen sulfide opens up a potential to infer sulfide concentrations in ancient anoxic basins via Mo isotope analysis (Arnold et al., 2012). However, both seawater δ^{98}Mo and bottomwater sulfide concentrations can change independently as a result of redox changes in local basins versus changes in the global oceanic Mo sinks.

Therefore, the scatter in the δ^{98}Mo record of euxinic sediments through time is not surprising, and the ambiguity currently complicate efforts to infer the secular evolution of seawater Mo isotope composition through time (e.g., see Kendall et al., 2017 for a recent summary). Currently, only the maximum δ^{98}Mo value from any one euxinic sedimentary succession is thought to represent seawater isotope composition, because isotope fractionation processes produce sediments with negative isotope offsets compared to overlying seawater (Dahl et al., 2010b; Kendall et al., 2015). However, this approach limits our ability to reconstruct secular changes in seawater composition, and we loose valuable information about bottomwater sulfide concentrations in the paleobasin that might be extracted from the geological record.

1.2. Aquatic molybdenum geochemistry

In current models for the Mo burial pathway(s) in euxinic settings, molybdenum is sourced as MoO_4^{2-} in oxic surface waters and ultimately ends in the sediments as reduced Mo(IV)-sulfides complexed with organic matter and/or Fe-sulfides in the sediments (Chappaz et al., 2014; Dahl et al., 2013a, 2016; Freund et al., 2016; Helz et al., 1996). The intermediate steps have not yet been identified in nature, but they seem to include sulfidation, reduction and scavenging with particulate matter.

In aqueous sulfidic solutions molybdate reacts with hydrogen sulfide to form thiomolybdates ($MoO_4^{2-} + H_2S \rightarrow MoO_{4-x}S_x^{2-} + H_2O$). When H_2S > 11 μM (= 100 μM total sulfide at pH = 8.1) the stable dissolved Mo species is MoS_4^{2-} (Erickson and Helz, 2000). However, these sulfidation reactions are rather slow. In sulfidic waters with 50 μM H_2S (comparable to Saanich Inlet or Cariaco Basin) it would take > 1 year for molybdate to react to tetrathiomolybdate and become the dominant species. Each successive sulfidation reaction is 10-fold slower than the previous reaction, suggesting sulfidic solutions evolve with only two consecutive thiomolybdate species predomiant at any point in time (if no other species-selective reactions occur) (Erickson and Helz, 2000). These sulfidation reactions impart strong Mo isotope fractionation (Tossell, 2005; Kerl et al., 2017) that can result in a net isotope offset between sediments and overlying seawater Mo removal, assuming the more sulfurized species are more particle reactive and are thus preferentially buried in the sediments (Amini et al., 2016; Arnold et al., 2004; Dahl et al., 2010a; Nägler et al., 2011).

Although, thiomolybdate is often said to be “particle reactive” (Lyons et al., 2009), Vorlicek et al., 2004 showed from laboratory experiments that the particle reactivity significantly increases when a reductant is added to thiomolybdate solutions. They found evidence that tri-thiomolybdate ($Mo^{VI}OS_3^{2-}$) reacts with zero-valent sulfur to form Mo^{IV}-polysulfide compounds and that the reduced phase can be readily scavenged from solution by pyrite (Vorlicek et al., 2004). We note that other reductants may also reduce Mo, and that other mineral surface including FeS, various clay minerals, and particulate organic matter also scavenge particle reactive Mo phases that form in aqueous sulfidic solution (Bertine, 1972; Bostick et al., 2003; Dahl et al., 2016; Helz et al., 2004; Vorlicek and Helz, 2002; Wagner et al., 2017).

Another potential fractionation process is Mn and Fe recycling at the O_2/H_2S chemocline. Molybdenum with a distinctly low δ^{98}Mo signature might adsorb onto Fe- and Mn-oxide mineral particles in the oxic zone (Noordmann et al., 2015; Scholz et al., 2013). Molybdenum will be released during reductive dissolution of the metal oxides once these settle into the sulfidic zone. As Mn^{2+} and Fe^{2+} diffuse back upwards into the oxic zone, fresh metal oxides will form and capture more Mo. This Fe-Mn cycling could potentially pump *molybdenum into the anoxic zone*. This process operates in sediments near the chemocline in the Baltic Sea (Scholz et al., 2013), where it produces substantial Mo enrichments (1–25 ppm) in the underlying sulfidic sediments relative to crustal rocks (but smaller enrichments than most sediments deposited in deep euxinic settings; i.e., 30–200 ppm) (Dahl et al., 2013b; Scott and Lyons, 2012). It may also be responsible for the low δ^{98}Mo signatures observed in the unstably euxinic parts of the Baltic Sea (Nägler et al., 2011; Noordmann et al., 2015; Scholz et al., 2013) and perhaps also in the mildly sulfidic sediments of the shallow parts of the Black Sea (Neubert et al., 2008). However, Mo isotope systematics in fully sulfidic basins shows that Mn-oxide cycling delivers only a minor proportion of the Mo present in the sulfidic deep waters and sediments, since neither sediments nor sulfidic waters carry lower δ^{98}Mo than overlying oxic waters (e.g., > 100 μM H_2S) (Dahl et al., 2010a; Nägler et al., 2011; Noordmann et al., 2015).

In this study, we find sediments deposited both under a range of H_2S concentrations and use various elemental and Mo speciation analyses to constrain the Mo burial pathway in a highly restricted setting.

1.3. Study site

We studied Mo burial pathways and isotopic signatures in Holocene sediments from the anoxic and sulfidic *Lake Cadagno*, situated in the Swiss Alps. Today, Lake Cadagno is permanently stratified with anoxic and sulfidic waters from ~11 to 21 m depth as a result of microbial sulfate reduction in the poorly ventilated deep waters (Del Don et al., 2001). Modern Mo isotope dynamics and Mo burial pathways operating from the oxic waters to the sediments have been studied in detail (Dahl et al., 2010a, 2013a). Total sulfide concentrations ($\Sigma S(-II) = H_2S + HS^- + S^{2-}$) reach 175–275 μM in the deepest part of the water column (21 m), and this sustains an anoxic phototrophic community of green and purple sulfur bacteria (Dahl et al., 2010a; Gregersen et al., 2009; Habicht et al., 2011; Musat et al., 2008; Tonolla et al., 2005). The pH below the chemocline is ~7.1 and temperature is ~4 °C, which means 110–190 μM of the total sulfide is dissociated into H_2S (Dahl et al., 2010a; Del Don et al., 2001). Sulfate is supplied mainly via subaquatic springs sourced from gypsum-rich dolomite bedrock (Del Don et al., 2001). Molybdenum is sourced both via rivers and subaquatic springs in roughly equal proportions, but with distinct Mo isotope signatures ($\delta^{98}Mo_{rivers}$ = 0.8 ± 0.1‰, $\delta^{98}Mo_{dolomite}$ = 1.5 ± 0.1‰, see definition of δ^{98}Mo below) (Dahl et al., 2010a). The euxinic conditions were established ~9800 years ago according to new geochemical and molecular evidence from a 10 m-long sediment core recovered from the deepest part of the lake (Wirth et al., 2013). Sedimentological evidence shows that intervals with frequent underflows triggered by flood events and injecting O_2-rich waters into deep sulfidic waters occurred in the course of the Holocene. Most striking is the period from 5000 to 1200 cal yr BP; it is characterized by the interval with peak flood frequencies from 4500 to 2400 cal yr BP and includes episodes with intermediate flood activity preceding and following the peak interval (Fig. 1d). The frequent occurrence of the flood-triggered underflows might

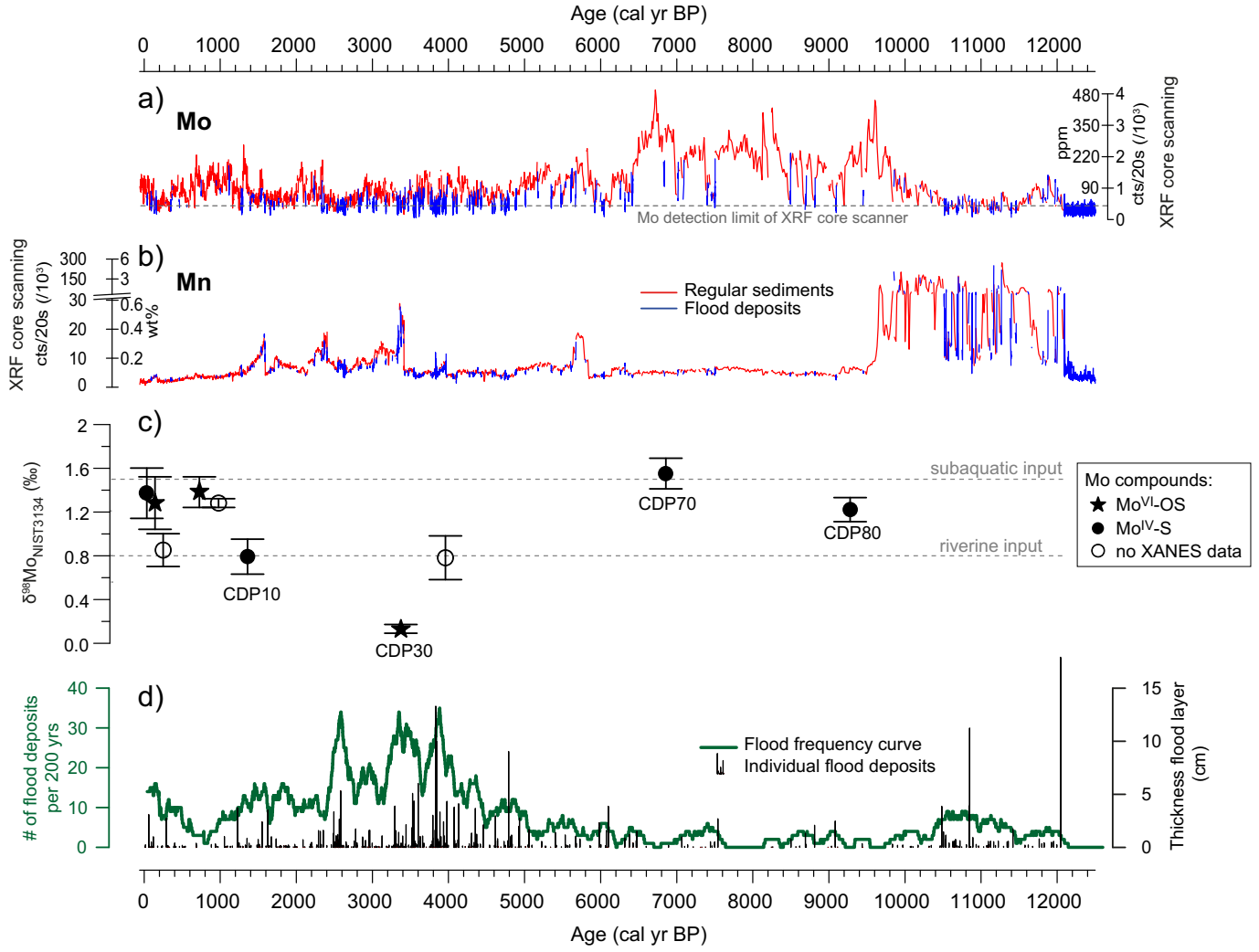

Fig. 1. Temporal evolution of geochemical and environmental properties of the Lake Cadagno sediments: a) Mo and (b) Mn concentrations in regular sediments and flood deposits from XRF (X-ray absorption fluorescence spectroscopy) core scanning at 1 mm down-core resolution (qualitative XRF core scanner counts calibrated by ICP-MS); c) δ^{98}Mo values and Mo speciation of discrete samples with horizontal dashed lines indicating the δ^{98}Mo values of the major water sources, river water and subaquatic sources; d) frequency of floods injecting O_2- and sediment-rich waters into the anoxic water column and recorded as flood deposits in the sediment sequence. For details on the data sets shown in (a), (b) and (d) refer to Wirth et al., 2013. In this time plot, samples containing mass-movement deposits are not represented (e.g., CDP8) as these event deposits are out of chronological order with the here represented regular sediments and flood deposits.

have interrupted or weakened the redox stratification in the lake and slightly lowered Mo content in the sediments (Wirth et al., 2013). This scenario differs from former results from recent sediments (until a sediment depth of 30 cm covering the past 150–200 years; Dahl et al., 2010a) recording a δ^{98}Mo signature indistinguishable from the source fluids to the lake, which is characteristic of deposition under highly euxinic conditions (with > 10 μM H_2S in the water column) (Arnold et al., 2012; Dahl et al., 2010a; Nägler et al., 2011; Neubert et al., 2008).

2. Samples and methods

We analyzed the Mo concentration and isotope composition in 21 samples from a 10 m-long sediment core collected at the deepest point of Lake Cadagno, i.e., at the depositional center. A subset of the samples was previously studied for Mo speciation using XAFS spectroscopy (Dahl et al., 2013a), and additional Mo-XANES characterizations of some samples are reported here. Sedimentological characterization, age determinations and mm-scale trace metal concentration analyses were performed on a parallel reference core (Wirth et al., 2013). The reference core was also used for detailed sedimentological descriptions, organic matter characterization, ^{14}C-, ^{137}Cs- and ^{210}Pb-dating and age-depth modeling (Wirth et al., 2013). The sediments consist of mainly three lithologies: 1) regular autochtonous sediment (RS) consisting of black laminated sediments with 8–16 wt% total organic carbon, 2) mass-movement deposits (MMD) consisting of sediment relocated from shallower depths in the lake to the depositional center, and 3) flood deposits (FD) with larger grains, high mineral content (gneissic signature), and organic matter almost exclusively of terrestrial origin.

The sediment cores were brought to the field station laboratory and were subsampled in 4 cm (short core, SC) and 10 cm intervals (long core, CDP), transferred to 50 mL centrifuge tubes and immediately frozen to − 20 °C to minimize oxidation prior to XAFS analyses. On average, the regular sediment samples represent intervals of ~40 years of sedimentation for the past 100 years and up to several hundred years for older sediments (Wirth et al., 2013). In comparison, the modern-day residence time of Mo in the sulfidic part of the lake is ~80–130 days (Dahl et al., 2010a). Thus, each sediment sample used for this study represents numerous seasons and/or cycles of Mo sedimentation rather than any single episodic event.

Elemental concentration data (incl. Mo, U, Mn, Fe and Al) were obtained at the Center for the Environment, Harvard University. Samples were digested with doubly distilled concentrated HNO_3 + HF (3:1) using a closed system Teflon vessel PicoTrace Dissolution unit. Concentrations were measured on aliquots diluted with 18.2 MΩ deionized H_2O on an

inductively coupled plasma mass spectrometer (ICP-MS) using a multi-element external standard solution, corrected for drift during analysis using an internal element spike (Ge, Y, In, Bi) at a constant level in all standards and sample solutions.

Mo isotope compositions were determined at Arizona State University by multiple-collector ICP-MS (Thermo Neptune®) using a calibrated $^{97}Mo + ^{100}Mo$ double spike to correct for instrumental mass bias according to the analytical procedure described in Goldberg et al. (2013). The molybdenum stable isotope composition is reported in terms of $\delta^{98}Mo$ notation where relative $^{98}Mo/^{95}Mo$ variability is reported in parts per thousand on a scale where the standard NIST-SRM 3134 is defined with $\delta^{98}Mo = 0.25‰$ (Nägler et al., 2013). On this scale, our in-house molybdenum standard, RochMo-2, gives $-0.09 \pm 0.05‰$, and open ocean oxic seawater is $\delta^{98}Mo = 2.34 \pm 0.10‰$ (Goldberg et al., 2013; Nägler et al., 2013).

X-Ray Absorption Near-Edge Spectroscopy (XANES) measurements were made at the MAX-II laboratory (Lund University, Sweden) at the superconducting multi-pole wiggler beam line i811 with 1.5 GeV beam energy and 100–200 mA electron current. Mo K-edge (20,000 eV) spectra were recorded using a Vortex Be 1 element fluorescence detector in steps of 5, 0.5 and 1.5 eV before the edge (−200 to −40 eV), at the edge (−40 to +60 eV), and after the edge (60 to 600 eV), respectively. Samples were thawed, dried and ground using an agate mortar and pestle in an anaerobic chamber at the NanoChalk Center, University of Copenhagen, before the sediments were packed in sample holders with Kapton tape windows and transported to the beamline in an anaerobic jar. The samples were only briefly (< 10 min) exposed to air before analysis during sample installation into the He-cooled cryostat. The energy scale was calibrated by simultaneously measuring Mo(0) foil in transmission mode, where the first three peaks in the derivative spectra of the Mo(0) foil were assigned 20,000.0, 20,010.5, and 20,024.0 eV (Dahl et al., 2013a; Wichard et al., 2009). Despite lower beam intensity at MAX-II and lower energy resolution using the Si(111) monochromator compared to previous data obtained at other beamlines (see below), we were able to distinguish XANES spectra for Mo-OS and Mo—S compounds (Fig. 2) and determine Mo oxidation states of the samples (Table 1) (Dahl et al., 2013a, 2016). Characteristic absorption peaks and edges were determined by spectral analysis in Matlab (Table 1).

XANES spectra were recorded at i811 for a set of reference materials and a set of new sediment samples (see Table 1). Some of the synthetic and natural reference materials ($Mo^{V}_{2}S_{8}$, $Mo^{IV}S_{2}$, Lake Cadagno: SC5 and CDP70) were previously analyzed at National Synchrotron Light Source (NSLS) at Brookhaven National Laboratories (beamlines X11-A, respectively Table 1). In addition, two new reference materials were analyzed; one Mo(V)-containing mineral, ilsemannite ($Mo_3O_8 \cdot nH_2O$, #1976.107) from the mineral collection at the Natural History Museum of Denmark and a natural molybdenite reference material from China (HLP-5). Our data showed that Mo K-edge XANES spectroscopy accurately determines the Mo oxidation state (± 0.4 unit) within the level of precision that E_K (± 1 eV) that was determined at i811 using a Si(111) monochromator crystal with lower energy resolution than at NSLS. New sediment samples analyzed in this study include two sediment samples from Lake Cadagno (CDP8, CDP10) with low $\delta^{98}Mo$, and two Devonian black shale samples with distinct $\delta^{98}Mo$ values of 1.84 ± 0.14‰ (Chattanooga shale, Chat2) and 1.05 ± 0.14‰ (Devonian Ohio Shale, SDO-1), respectively (Dahl et al., 2010b; Goldberg et al., 2013).

3. Results

3.1. Molybdenum concentrations and isotopes

The Cadagno drill core samples display a strong relationship between Mo concentrations and $\delta^{98}Mo$ (Fig. 3). Sediments with the highest Mo concentrations of 100–200 ppm are associated with a distinct narrow range of high $\delta^{98}Mo$ values (1.2–1.5‰), corresponding to the properties of the modern surface sediments (120–180 ppm Mo; $\delta^{98}Mo$ = 1.2–1.4‰; Dahl et al., 2010a). Five out of seven samples consisting partly or fully of mass-movement material have Mo concentrations < 25 ppm, but cover a large range of $\delta^{98}Mo$ values (Fig. 3). This allows evaluating the relative contribution of allochthonous (ALL) and autochthonous (AUT) sediments to the mass-movement material. Allochthonous sediment derived from the oxic zone defines one end-member composition on a mixing curve carrying low Mo contents and low $\delta^{98}Mo$ values (Mo ~ 2–4 ppm, $\delta^{98}Mo_{ALL}$ ~ 0.1–0.4‰) whereas the other component is autochthonous euxinic sediments with high Mo and high $\delta^{98}Mo$ (> 100 ppm, $\delta^{98}Mo_{AUT} = 1.4 \pm 0.1‰$). We define the dilution factor from the Mo isotope composition of the sediment: $f_{DIL} = (\delta^{98}Mo_{AUT} - \delta^{98}Mo) / (\delta^{98}Mo_{AUT} - \delta^{98}Mo_{ALL})$. The two remaining samples recognized as consisting partly of mass-movement material, do not show a diluted signal (CDP70, CDP80), likely because sediment was transported from within the anoxic-sulfidic zone (this is also visually apparent by intermixed fragments of regular sediment).

Three samples (CDP8, CDP10, and CDP30) fall significantly below the

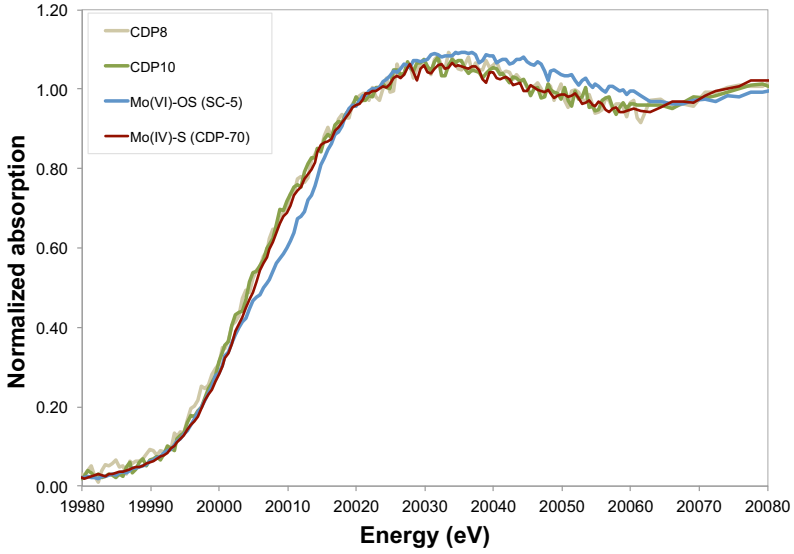

Fig. 2. Molybdenum XANES spectra of $\delta^{98}Mo$-fractionated samples CDP8 and CDP10 compared to samples with predominant Mo^{IV}-S (CDP70) and Mo^{VI}-OS (SC5) compounds for illustrating the Mo^{IV}-S character of CDP8 and CDP10. All data was obtained at the MAX-II laboratory (Lund University, Sweden) i811 beamline. Peak and edge energies are tabulated in Table 1.

Table 1
Diagnostic XANES features for reference materials and samples. E_K: K-edge, E_M: Maximum absorption beyond K-edge and Pre-edge inflection point. Signal analysis of the XANES spectra was performed in Matlab using a smoothing spline fit to calculate derivative spectra (for details, see Dahl et al., 2013a). Uncertainties greater than this were calculated from comparing spline fits with various smoothing factors ρ (range shown), where ρ = 0 and ρ = 1 corresponds to a perfectly smooth curve and a curve close to data (no smoothing), respectively.

	E_K	E_M	E_M - E_K	Pre-edge inflection	Scans	ρ	Beamline
Reference material							
MoS_2	6.1	30.1	24	–	4	0.8	X11-A
MoS_2	5.3 ± 1.0	30.5 ± 1.0	25.2 ± 1.0	–	3	0.2–0.4	i811
Mo_2S_8	9 ± 1	35 ± 1	26 ± 1	−0.3 ± 1.0	3	0.5	X11-A
Mo_2S_8	8.5 ± 1.0	39.0 ± 3.8	30.5 ± 3.9	1.2 ± 1.0	5	0.1–0.4	i811
Mo^{VI}-OS sediment (SC-5)	16.9	36.5	19.6	1.8	5	0.5	X11-A
Mo^{VI}-OS sediment (SC-5)	14.4 ± 1.0	35.2 ± 1.0	20.8 ± 1.0	0.8 ± 1.0	11	0.2–0.4	i811
Mo^{IV}-S sediment (CDP-70)	6.6	31.4	24.8	–	4	0.5	X11-A
Mo^{IV}-S sediment (CDP-70)	5.2 ± 1.0	31.6 ± 3.3	26.5 ± 3.4	–	11	0.2–0.4	i811
Samples and new standards							
CDP8-X	8.2 ± 1.7	33.3 ± 1.0	25.1 ± 2.0	–	10	0.5–0.7	i811
CDP10-X	8.3 ± 1.0	33.7 ± 1.3	25.4 ± 1.6	–	5	0.6–0.8	i811
Chattanooga shale (Chat 2)	14.6 ± 1.0	33.3 ± 1.0	18.7 ± 1.4	2.5 ± 1.0	11	0.2–0.4	i811
Devonian Ohio Shale (SDO-1)	14.1 ± 1.0	33.3 ± 1.0	19.2 ± 1.4	3.7 ± 1.0	9	0.2–0.4	i811
Molybdenite ore from China (HLP-5)	3.7 ± 1.0	31.1 ± 1.2	27.4 ± 1.6	–	6	0.2–0.4	i811
Ilsemannite, $Mo_3O_8{\cdot}nH_2O$ (1976.107)	15.3 ± 1.0	36.1 ± 1.0	20.8 ± 1.4	1.8 ± 1.0	6	0.2–0.4	i811

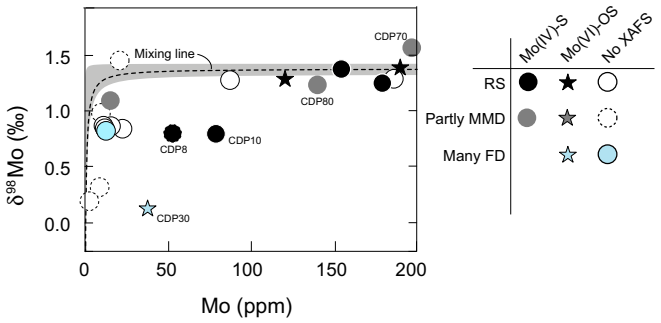

Fig. 3. Sedimentary Mo content versus δ^{98}Mo in bulk sediment samples from Lake Cadagno with symbols representing sedimentary lithology and predominant Mo speciation, obtained with XAFS (see legend). The mixing curves are set by two end member compositions (Mo, δ^{98}Mo) representing oxic sediments/detrital material (2–10 ppm, 0.0–0.4‰) and highly euxinic sediments with unfractionated Mo (200 ppm, 1.35–1.55‰), respectively. The shaded area represents the uncertainties of end member compositions.

mixing curves in a plot of δ^{98}Mo versus Mo concentration (Fig. 3). CDP30 and CDP10 were deposited during flood-rich periods, and CDP8 contains remobilized sediments possibly originally deposited during flood-rich periods (Table 2). In detail, CDP30 consists of a mixture of regular autochthonous sediment deposited in the deepest part of the lake and washed-in allochthonous flood material; CDP10 consists of regular autochthonous sediments; and CDP8 consists at least in part of mass-movement material transported from the oxic zone. In principle, a higher proportion of riverine Mo to the lake (with $\delta^{98}Mo_{rivers}$ = 0.8 ± 0.1‰) relative to Mo from subaquatic springs (1.5 ± 0.1‰) could shift δ^{98}Mo of the sediments to lower values, i.e., producing the signatures of CDP8 and CDP10 (δ^{98}Mo = 0.79 ± 0.15‰ and 0.79 ± 0.16‰, respectively) (Dahl et al., 2010a; all published data was recalculated to the NIST SRM 3134 scale; Table 2). However, one sample (CDP30) carries even lower δ^{98}Mo (0.13 ± 0.04‰) than can be accommodated by a greater proportion of riverine input relative to subaquatic spring water in the lake. Also, we note that it is difficult to maintain euxinic conditions in the lake if the mixing ratio of riverine water to ground water was high enough to result in δ^{98}Mo ~ 0.8‰, since sulfate (for sulfide production) is supplied almost exclusively from the subaquatic springs. Alternatively, Mo adsorbed onto Mn-oxides with a low δ^{98}Mo was sourced into the sediments at these times, and/or Mo isotope fractionation occurred during the Mo removal process. In any case, these three samples contain Mo products that were isotopically fractionated in the lake. Mo was not quantitatively removed from the water column when these sediments formed and a substantial portion of Mo transported across the chemocline must have escaped via the oxic water column.

There is a positive correlation between sedimentary Mo and U concentrations; in which undiluted samples simultaneously display both higher Mo and U enrichments, which in turn are comparable to sediments deposited in other anoxic and euxinic marine settings (Fig. 4). The undiluted δ^{98}Mo-unfractionated samples display systematically higher average molar Mo/U ratio (7.7 ± 2.1) than diluted samples (3.3 ± 1.3) and dissolved Mo/U ratio in oxic lake water (Mo/U = 4.0 ± 0.4; calculated from Mo = 12.5 ± 1.0 nM, U = 3.2 ± 0.2 nM; Dahl et al., 2010a). The δ^{98}Mo-fractionated samples have only slightly elevated Mo/U values (5.3 ± 1.2), but this is due to one sample, CDP8, with a low Mo/U value (3.9) recognized as a mass-movement deposit.

3.2. Molybdenum speciation

XANES spectra at the Mo K-edge allow us to assess the Mo oxidation state (E_K) and the immediate bonding environment (e.g., Mo═O, Mo−O, Mo−S) in both amorphous and crystalline Mo compounds. This principle is illustrated in a simplified manner in Fig. 5, where our new reference material, Mo_3O_8, falls at the correct E_K value (15.3 ± 1.0) between that of $Mo^{IV}O_2$ (11.9) and $Mo^{VI}O_4^{2-}$ (16.8) corresponding to an average oxidation state of 5.4 ± 0.4 indistinguishable from its formal oxidation state (5.33) (Dahl et al., 2013a).

Two of the δ^{98}Mo-fractionated samples (CDP8 and CDP10) display average Mo oxidation states of ~4 and Mo−S as the principle ligands, indistinguishable from other Mo^{IV}-S compounds in the lake sediments (e.g., CDP70) (Fig. 5). This result is robust even though it has not been possible to validate the structure from the EXAFS spectra obtained at i811. Therefore, we make the important observation that the Mo^{IV}-S structure is not diagnostic of a quantitative Mo removal pathway and δ^{98}Mo-unfractionated sediments.

Several samples display XANES spectra similar to oxidized Mo^{VI}-OS compounds (star symbols in Figs. 1 and 3), and there is also no systematic relationship to their Mo isotope composition. For example, the δ^{98}Mo-fractionated sample CDP30 carries a strong signal of Mo═O bonds (Dahl et al., 2013a), whereas several unfractionated samples also contain predominantly Mo^{VI}-OS compounds. Post-depositional oxidation can produce oxidized Mo compounds without affecting the Mo isotope composition. That said – it is still possible that the oxidized Mo compounds precipitated directly in the lake via a pristine removal pathway (Dahl et al., 2013a).

Table 2
Sedimentological and chemical characteristics of the Lake Cadagno drill core samples. The sedimentological description and the age-depth model are described in Wirth et al. (2013). Mo speciation (XAFS) analyses are described in (Dahl et al., 2013a). Samples containing material from mass-movement deposits (MMD) are shown in grey.

Name	Lithology	Depth (cm)	Age (yr)	$\delta^{98}Mo_{NIST\text{-}SRM3134}$ ± 2SD (n) ‰[a]	Dilution f_{dil}[b]	XAFS type	Ca (wt%)[c]	Mn (ppm)[c]	Fe (wt%)[c]	Al (wt%)[c]	Mo (ppm)[c]	U ppm[c]
SC1	RS, few FD	−1 ± 2	0	1.23 ± 0.12 (4)	18%	Mo^{IV}-S	1.5	299	4.7	5.1	179	48
SC3	RS, few FD	7 ± 2	35	1.37 ± 0.23 (4)	7%	Mo^{IV}-S	1.4	648	6.2	5.1	155	42
SC5	RS, few FD	15 ± 2	143	1.28 ± 0.24 (4)	14%	Mo^{VI}-O-S	1.5	1149	6.0	5.3	120	30
CDP2	RS, few FD	53 ± 5		0.83 ± 0.08 (4)	51%		1.4	702	4.7	5.3	23	17
SC7	RS, few FD	23 ± 2	250	0.85 ± 0.15 (3)	49%		1.6	1544	6.4	5.5	11	7
CDP3	RS, few FD	63 ± 5		1.26 ± 0.01 (3)	16%		1.4	849	5.7	5.3	87	29
SC9	MMD	31 ± 2		0.31 ± 0.17 (4)	94%		1.6	1152	5.0	6.2	4	6
CDP4	Partly MMD	73 ± 5		1.44 ± 0.42 (3)	1%		1.7	1051	5.5	5.8	22	14
SC11	MMD	39 ± 2		0.81 ± 0.21 (4)	53%		1.7	685	4.8	7.0	12	7
CDP5	MMD	83 ± 5		0.98 ± 0.12 (3)	39%		1.7	827	5.0	5.6	10	9
CDP6	RS, few FD	93 ± 5	726	1.39 ± 0.14 (4)	5%	Mo^{VI}-O-S	1.2	1071	6.0	5.0	190	59
CDP7	RS, few FD	103 ± 5	978	1.28 ± 0.04 (3)	14%		1.4	1177	6.2	5.2	186	52
CDP8	MMD	113 ± 5		0.79 ± 0.15 (3)	Fractionated	Mo^{IV}-S	1.4	987	5.2	5.5	44	28
CDP9	RS (lots of MMD)	123 ± 5	1173			Mo^{IV}-S	1.6	1408	6.1	5.5	88	31
CDP10	RS	135 ± 5	1359	0.79 ± 0.16 (4)	Fractionated	Mo^{IV}-S	1.6	3148	5.7	5.5	73	32
CDP20	Partly MMD	236 ± 5	2005	1.08 ± 0.16 (3)	30%	Mo^{VI}-O-S	1.4	782	4.3	5.0	16	10
CDP25							1.7	1346	4.9	5.5	10	5
CDP30	RS (lots of FD, possibly some MMD)	365 ± 5	3374	0.13 ± 0.04 (2)	Fractionated	Mo^{VI}-O-S	1.7	2398	5.3	5.3	38	15
CDP40	Many (mostly) FDs	465 ± 5	3960	0.78 ± 0.20 (4)	55%		2.0	811	4.9	5.8	9	4
CDP50	MMD (mineral-rich, 'oxic deposition' likely)	566 ± 5		0.20 ± 0.01 (2)	100%		2.1	672	4.4	5.4	3	2
CDP60	MMD (fragments of RS, organic-rich rel. to CDP50)	691 ± 5		0.85 ± 0.22 (3)	49%		1.7	1824	5.6	6.9	8	11
CDP60 -rpt	–			0.83 ± 0.11 (3)	51%		1.6	1830	5.6	6.6	8	11
CDP70	Partly MMD (and FD and RS → mix)	782 ± 5	6857	1.55 ± 0.14 (3)	−8%	Mo^{IV}-S	1.7	1873	5.8	5.1	197	61
CDP80	Partly MMD (and FD and RS → mix)	884 ± 5	9279	1.22 ± 0.11 (3)	19%	Mo^{IV}-S	2.0	2119	5.4	5.5	140	78

[a] Mo isotope compositions are given in terms of the $^{98}Mo/^{95}Mo$ ratio relative to the global reference material, NIST-3134 with $\delta^{98}Mo_{NIST3134} = 0.25‰$. Our data was collected using the in-house RochMo-2 standard as reference material, so reported $\delta^{98}Mo_{NIST3134}$ values were re-calculated using $\delta^{98}Mo_{NIST3134} = \delta^{98}Mo_{RochMo2}$–0.09‰ (Goldberg et al., 2013).

[b] The dilution with end-member 1 (EM1) material was calculated for samples on a two-component mixing curve: $f_{dil} = [\delta^{98}Mo - \delta^{98}Mo_{EM1}] / [\delta^{98}Mo_{EM2} - \delta^{98}Mo_{EM1}]$, assuming isotope variation is due to mixing Mo-diluted material with 2–4 ppm Mo and $\delta^{98}Mo_{EM1} = 0.2–0.4‰$ (i.e., riverine sediments) into pristine authigenic euxinic sediment with ≥ 100 ppm Mo and $\delta^{98}Mo_{EM2} = 1.3–1.6‰$. The range of values leads to an estimated uncertainty of ± 26% (2SD). Therefore, undiluted samples are defined as $f_{dil} < 26\%$.

[c] Sample reproducibilty was better than < 5% (e.g., CDP60), and the accuracy was 15–25% determined using certified reference materials (SCO-1, BCR-2). Abbreviations: RS: regular sediment, MMD: mass movement deposit, FD: flood deposit, rpt = repeated digestion.

Previous EXAFS analyses have shown that black shales (euxinic mudrocks) contain Mo—O bonds (Helz et al., 1996). We add two Devonian shale samples with known $\delta^{98}Mo$ values to this database (Chat2: 1.84 ± 0.14‰; SDO-1; 1.05 ± 0.14‰). Both of these samples fall within the Mo—O array with an average oxidation state of ~5 (Fig. 5) similar to Mo-OS samples from Lake Cadagno. Therefore, these Devonian shales contain either a mixture of Mo(IV) and Mo(VI)-phases, exclusively Mo(V)-phases, or a combination of all. Again, we make the important observation that Devonian black shales with both high and low $\delta^{98}Mo$ contain Mo—O bonds. Hence, the predominant Mo species in

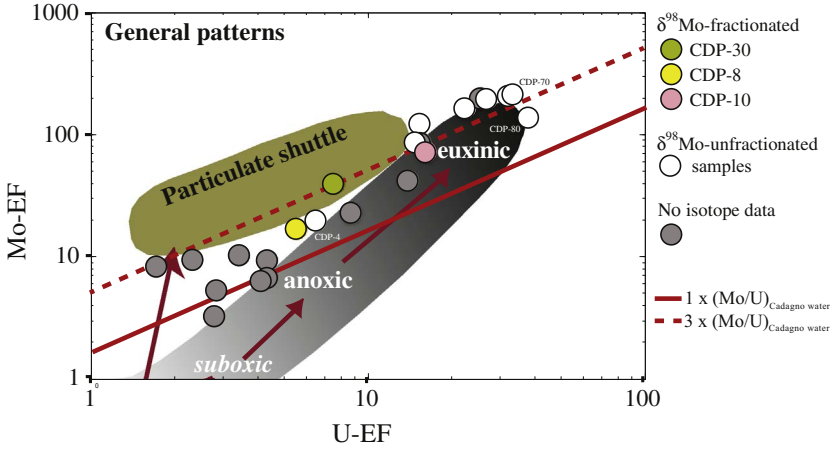

Fig. 4. Mo enrichments versus U enrichments calculated as X EF = $(X/Al)_{sample} / (X/Al)_{crust}$ (Taylor and McLennan, 1995) of the Lake Cadagno samples. Characteristic regions (suboxic, anoxic and euxinic) are corrected for the lower Mo/U in Lake Cadagno water compared to seawater (Tribovillard et al., 2012).

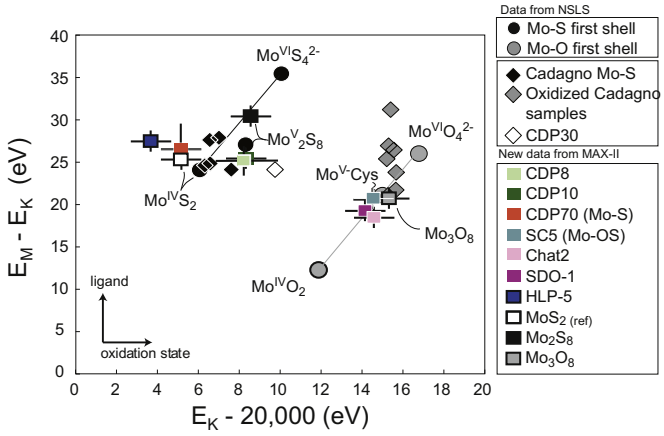

Fig. 5. Diagnostic features in the XANES spectra reveal a simple operational distinction between Mo—O vs. Mo—S bonding environments and oxidation state (Table 2). This relationship is manifested in data from reference materials and euxinic sediment samples measured at Brookhaven National Laboratory with beamline X11-A (diamonds) (Dahl et al., 2013a). Overall, synthetic (MoS_2, Mo_2S_8) and natural (CDP70, SC5) reference materials from Lake Cadagno, analyzed at the MAX-II lab i811 beamline (squares), reproduce E_K-values observed NSLS. However, a slightly higher E_M is observed for Mo_2S_8, but still within the Mo—S array. The Mo(V)-containing mineral, ilsemannite ($Mo_3O_8{\cdot}nH_2O$) has a formal Mo oxidation state of 5.33 and falls exactly on the expected Mo—O trend between Mo(IV)O_2 and Mo(VI)O_4^{2-}. A molybdenite ore sample from China (HLP-5) is found close to synthetic MoS_2, but at significantly lower E_K and higher E_M values. This offset may be taken as an estimate of the accuracy of the measurements at i811 using the Si(111) monochromator with lower energy resolution.

these sedimentary rocks are probably not diagnostic for Mo isotope fractionation processes occurring in their deposition environment.

4. Discussion

4.1. δ^{98}Mo-fractionation in Lake Cadagno ~3000 years ago

Dahl et al., 2010a, 2010b concluded that Mo isotope fractionation occurs in the sulfidic water column, but sediments display no net isotopic offset from lake sources due to quantitatively Mo removal from the water column to the sediments. Our new results confirm this behavior for most of the Holocene, but also show periods when Mo isotope fractionation was expressed in the Lake Cadagno sediments.

To understand how the δ^{98}Mo-fractionated samples (CDP8, CDP10, CDP30) from Lake Cadagno formed, it is worthwhile looking carefully into the context of the lake's environmental history as it has been discussed in Wirth et al. (2013). Notably, CDP30 was deposited during an episode of strongly increased flood frequency ~3400 years ago (Fig. 1d). These floods could have periodically interrupted the chemical stratification in the water column and ventilated the deep part of the lake. The periods with high flood frequency, during which CDP30 and also CDP10 (~1400 cal yr BP) were deposited, are associated with muted (but still high) Mo enrichments (~80 ppm, Fig. 1a) that are also indicative of mildly euxinic conditions in marine systems (Scott and Lyons, 2012). At the same time, molecular and DNA records suggest an ecological shift in the anoxygenic phototrophic community where green sulfur bacteria (GSB) started to dominate over purple sulfur bacteria (Wirth et al., 2013). GSB are generally agreed to cope better with dimmer light condition (Manske et al., 2005; Tonolla et al., 2005), for example at the time when flooding episodes would have frequently injected loose sediment from the catchment.

Two of three fractionated (CDP30, CDP10) samples have elevated Mn contents (2400 and 3150 ppm), whereas CDP8 (1000 ppm) is similar to average sediments (1300 ppm) (Table 2). CDP10 and CDP30 contain regular sediment, whereas CDP8 contains mass movement material that might well have been transported in the oxic zone. There is no Ca-Mn correlation at these deposition intervals, suggesting that precipitation of Mn-oxides, not Mn^{2+}-carbonates, occurred in the lake. This could be due to the injection of O_2-rich underflows at least during deposition of CDP30 and CDP10 (contrary to the Mn-enriched transition period from oxic to euxinic conditions > 9800 yrs ago (Wirth et al., 2013). CDP8 might have formed with no Mn enrichments (e.g., in the oxic part of the lake), or lost Mn-oxides and any enrichment signature during subsequent mass movement within the anoxic part of the lake, or perhaps Fe-oxides played a greater role on Mo scavenging. In any case, physical, biological and chemical lines of evidence are all supportive that the δ^{98}Mo-fractionated samples formed in the lake when hydrogen sulfide levels were (episodically) lower than today and perhaps with Mo contribution via Mn-oxide cycling when the O_2/H_2S chemocline was nearer the lake floor.

4.2. Do Mo speciation data discern isotope fractionation processes?

Although isotope fractionation is induced only between distinct Mo species (i.e., due to differences in bond strengths Anbar and Rouxel, 2007), there is no guarantee that the characteristic species involved in the fractionation process operating in the water column are preserved or leave any observable differences in the chemical structure of the sediments. The presence of δ^{98}Mo-fractionated and δ^{98}Mo-unfractionated samples along with two distinct chemical signatures in Lake Cadagno allowed us to explore such Mo isotope-speciation relationship further as well as to further constrain the euxinic Mo burial pathway.

First, it has already been established that post-depositional oxidation can alter the Mo speciation of the euxinic sediments, as it can produce the same Mo^{VI}-O signature in samples with predominant Mo^{IV}-S compounds (Dahl et al., 2013a). This will not change δ^{98}Mo unless Mo is lost or gained in the process. Indeed, some of our δ^{98}Mo-unfractionated samples contain predominantly Mo^{VI}-O compounds (Fig. 3) that could be ascribed to post-depositional oxidation (e.g., during retrieval of the core and transfer into the laboratory), and this process is also a reasonable explanation for the predominance of Mo^{VI}-O compounds in ancient euxinic outcrop samples (including SDO-1 and Chat-2 with distinct δ^{98}Mo signatures). Ultimately, our data cannot rule out the possibilities that either Mo^{VI}-OS or Mo^{IV}-S compounds directly precipitated in this euxinic basin.

Importantly, our data shows that Mo^{IV}-S compounds are not diagnostic for quantitative Mo removal and δ^{98}Mo-unfractionated euxinic sediments. This is clear from the observation that the bulk Mo^{IV}-S signature, in addition to Mo^{VI}-OS, is predominant among the δ^{98}Mo-fractionated samples. Either the Mo species involved in the Mo isotope fractionation process carry chemical differences not distinguished in the XAFS spectra (for example, isotope fractionation occurs between two distinct Mo^{IV}-S compounds) or the δ^{98}Mo-fractionated Mo compounds have been altered during subsequent processing of the reactive Mo compounds (e.g., dissolution and re-precipitation in the sulfidic zone). Given what we know about thiomolybdate reduction, it seems likely that the Mo=O bonds of reactive reduced Mo compounds, such as the Mo-polysulfide $Mo^{IV}O(S_4)S^{2-}$, are not preserved during subsequent processing (Vorlicek et al., 2004). Indeed, Dahl et al., 2010a, 2010b found evidence for Mo re-dissolution in the uppermost 15 cm of the sediments and used mass balance considerations to find a substantial Mo return flux (~20%) from the sediment towards the water column. As Mo re-dissolves from the solid phase and a slightly ^{98}Mo-depleted solute (− 0.2‰) enters the pore fluids. Eventually, the desorbed Mo will re-precipitate in the sediments where sulfide levels are higher ($\Sigma S(-II)$ = 500–1000 μM) and adsorption sites are more readily available than in the water column. This early diagenetic Mo recycling arguably occurred because the Mo host phase is diagenetically unstable, for example when (Mo associated) organic matter is remineralized and/or amorphous FeS is converted to pyrite. Therefore, we suggest that even if Mo^{VI}-OS compounds precipitated directly from the water column, then these could be reduced and Mo—S bonds could form during shallow diagenesis with only a small impact on δ^{98}Mo in

the sediments. Conclusively, the observed Mo speciation signatures do not discern isotope fractionation processes occurring in the lake.

5. Implications and future directions

The molybdenum isotope composition of ancient euxinic sediments is mainly a function of both globally integrated ocean oxygenation, bottom water hydrogen sulfide levels in ancient sulfidic basins, post-depositional mobilization processes and the Mo source to the sediments (e.g., Mn-oxides vs. seawater). However, there is currently no way to discriminate between these processes.

We proposed that Mo speciation data (as well as Mo concentrations, Mo/U) might reveal isotope fractionation process in euxinic settings. Data from a Holocene drill core through Lake Cadagno's sediments reject this assertion, but it is still possible that Mo compounds and/or other sedimentary metrics reveal fractionation processes at play in other euxinic systems; e.g., samples that have not suffered from post-depositional oxidation or post-reductional sulfidation. In this context, it is particular important to study less restricted marine euxinic settings, including intermittently sulfidic upwelling zones on the continental shelves, in which Mo burial is limited by the rate of thiomolybdate formation relative to water renewal in the basin. With more molybdenum speciation and isotope data from a wider range of euxinic environments, we would better understand the intermediate chemical steps in the Mo burial process and evaluate the tantalizing prospect of using Mo isotopes as a dual recorder of both global ocean oxygenation and hydrogen sulfide levels in local paleo-basins.

Acknowledgments

All Mo analyses were performed at the W.M. Keck Foundation Laboratory for Environmental Biogeochemistry and thanks are extended to Gwyneth W. Gordon and Ariel D. Anbar for their help and encouragement in the laboratory. Moritz Lehmann and Adrian Gilli assisted with sample collection during fieldwork. Knud Dideriksen and Susan Stipp from the Chemistry Department, University of Copenhagen, kindly provided access to anaerobic chambers. Beamline scientist Stefan Carlson instructed XAFS analyses at MAX-II lab. Zina Fihl and Tonci Balic-Zunic provided a piece of ilsemannite from the mineral collection at the Natural History Museum Denmark. Tom Weber and Jarl A. Boyd assisted with the XANES analyses at the beamline. TWD thanks Stephen Romaniello, Anthony Chappaz, Trent Vorlicek, Andy Knoll, and Don Canfield for helpful assistance and fruitful discussions. Financial support was supplied to TWD from the Villum Foundation (VKR023127 and ID1168439) and Danish National Research Foundation (DNRF-53, Nordic Center for Earth Evolution). S.B.W. thanks the Swiss National Science Foundation for financial support (Grants 121909 and 137930).

References

Amini, M., Weis, D., Soon, M., Francois, R., 2016. In: Molybdenum isotope fractionation in Saanich Inlet. Goldschmidt Conference, Yokohama, Japan. British Columbia.
Anbar, A.D., Rouxel, O., 2007. Metal stable isotopes in paleoceanography. Annu. Rev. Earth Planet. Sci. 35, 717–746.
Arnold, G.L., Anbar, A.D., Barling, J., Lyons, T.W., 2004. Molybdenum isotope evidence for widespread anoxia in mid-proterozoic oceans. Science 304, 87–90.
Arnold, G.L., Lyons, T.W., Gordon, G.W., Anbar, A.D., 2012. Extreme change in sulfide concentrations in the Black Sea during the Little Ice Age reconstructed using molybdenum isotopes. Geology 40, 595–598.
Baldwin, G.J., Nägler, T.F., Greber, N.D., Turner, E.C., Kamber, B.S., 2013. Mo isotopic composition of the mid-Neoproterozoic ocean: an iron formation perspective. Precambrian Res. 230, 168–178.
Barling, J., Arnold, G.L., Anbar, A.D., 2001. Natural mass-dependent variations in the isotopic composition of molybdenum. Earth Planet. Sci. Lett. 193, 447–457.
Bertine, K., 1972. The deposition of molybdenum in anoxic waters. Mar. Chem. 1, 43–53.
Bostick, B.C., Fendorf, S., Helz, G.R., 2003. Differential adsorption of molybdate and tetrathiomolybdate on pyrite (FeS_2). Environ. Sci. Technol. 37, 285–291.
Chappaz, A., Lyons, T.W., Gregory, D.D., Reinhard, C.T., Gill, B.C., Li, C., Large, R.R., 2014. Does pyrite act as an important host for molybdenum in modern and ancient euxinic environments? Geochim. Cosmochim. Acta 126, 112–122.
Chen, X., Ling, H.F., Vance, D., Shields-Zhou, G.A., Zhu, M., Poulton, S.W., Och, L.M., Jiang, S.Y., Li, D., Cremonese, L., Archer, C., 2015. Rise to modern levels of ocean oxygenation coincided with the Cambrian radiation of animals. Nat. Commun. 6, 7142.
Dahl, T.W., Anbar, A.D., Gordon, G.W., Rosing, M.T., Frei, R., Canfield, D.E., 2010a. The behavior of molybdenum and its isotopes across the chemocline and in the sediments of sulfidic Lake Cadagno, Switzerland. Geochim. Cosmochim. Acta 74, 144–163.
Dahl, T.W., Hammarlund, E.U., Anbar, A.D., Bond, D.P.G., Gill, B.C., Gordon, G.W., Knoll, A.H., Nielsen, A.T., Schovsbo, N.H., Canfield, D.E., 2010b. Devonian rise in atmospheric oxygen correlated to the radiations of terrestrial plants and large predatory fish. Proc. Natl. Acad. Sci. 107, 17911–17915.
Dahl, T.W., Canfield, D.E., Rosing, M.T., Frei, R.E., Gordon, G.W., Knoll, A.H., Anbar, A.D., 2011. Molybdenum evidence for expansive sulfidic water masses in ~750 Ma oceans. Earth Planet. Sci. Lett. 311, 264–274.
Dahl, T.W., Chappaz, A., Fitts, J.P., Lyons, T.W., 2013a. Molybdenum reduction in a sulfidic lake: evidence from X-ray absorption fine-structure spectroscopy and implications for the Mo paleoproxy. Geochim. Cosmochim. Acta 103, 213–231.
Dahl, T.W., Ruhl, M., Hammarlund, E.U., Canfield, D.E., Rosing, M.T., Bjerrum, C.J., 2013b. Tracing euxinia by molybdenum concentrations in sediments using handheld X-ray fluorescence spectroscopy (HHXRF). Chem. Geol. 360–361, 241–251.
Dahl, T.W., Chappaz, A., Hoek, J., McKenzie, C.J., Svane, S., Canfield, D.E., 2016. Evidence of molybdenum association with particulate organic matter under sulfidic conditions. Geobiology 1–13.
Del Don, C., Hanselmann, K.W., Peduzzi, R., Bachofen, R., 2001. The meromictic alpine Lake Cadagno: orographical and biogeochemical description. Aquat. Sci. 63, 70–90.
Dickson, A.J., Cohen, A.S., Coe, A.L., 2014. Continental margin molybdenum isotope signatures from the early Eocene. Earth Planet. Sci. Lett. 404, 389–395.
Duan, Y., Anbar, A.D., Arnold, G.L., Lyons, T.W., Gordon, G.W., Kendall, B., 2010. Molybdenum isotope evidence for mild environmental oxygenation before the Great Oxidation Event. Geochim. Cosmochim. Acta 74, 6655–6668.
Erickson, B.E., Helz, G.R., 2000. Molybdenum(VI) speciation in sulfidic waters: stability and lability of thiomolybdates. Geochim. Cosmochim. Acta 64, 1149–1158.
Freund, C., Wishard, A., Brenner, R., Sobel, M., Mizelle, J., Kim, A., Meyer, D.A., Morford, J.L., 2016. The effect of a thiol-containing organic molecule on molybdenum adsorption onto pyrite. Geochim. Cosmochim. Acta 174, 222–235.
Goldberg, T., Gordon, G., Izon, G., Archer, C., Pearce, C.R., McManus, J., Anbar, A., Rehkämper, M., 2013. Resolution of inter-laboratory discrepancies in Mo isotope data: an intercalibration. J. Anal. At. Spectrom.
Gordon, G.W., Lyons, T.W., Arnold, G.L., Roe, J., Sageman, B.B., Anbar, A.D., 2009. When do black shales tell molybdenum isotope tales? Geology 37, 535–538.
Gregersen, L.H., Habicht, K.S., Peduzzi, S., Tonolla, M., Canfield, D.E., Miller, M., Cox, R.P., Frigaard, N.U., 2009. Dominance of a clonal green sulfur bacterial population in a stratified lake. FEMS Microbiol. Ecol. 70, 30–41.
Habicht, K.S., Miller, M., Cox, R.P., Frigaard, N.-U., Tonolla, M., Peduzzi, S., Falkenby, L.G., Andersen, J.S., 2011. Comparative proteomics and activity of a green sulfur bacterium through the water column of Lake Cadagno, Switzerland. Environ. Microbiol. 13, 203–215.
Helz, G.R., Miller, C.V., Charnock, J.M., Mosselmans, J.F.W., Pattrick, R.A.D., Garner, C.D., Vaughan, D.J., 1996. Mechanism of molybdenum removal from the sea and its concentration in black shales: EXAFS evidence. Geochim. Cosmochim. Acta 60, 3631–3642.
Helz, G.R., Vorlicek, T.P., Kahn, M.D., 2004. Molybdenum scavenging by iron monosulfide. Environ. Sci. Technol. 38, 4263–4268.
Herrmann, A.D., Kendall, B., Algeo, T.J., Gordon, G.W., Wasylenki, L.E., Anbar, A.D., 2012. Anomalous molybdenum isotope trends in Upper Pennsylvanian euxinic facies: significance for use of δ^{98}Mo as a global marine redox proxy. Chem. Geol. 324–325, 87–98.
Kendall, B., Creaser, R.A., Gordon, G.W., Anbar, A.D., 2009. Re–Os and Mo isotope systematics of black shales from the Middle Proterozoic Velkerri and Wollogorang Formations, McArthur Basin, northern Australia. Geochim. Cosmochim. Acta 73, 2534–2558.
Kendall, B., Gordon, G.W., Poulton, S.W., Anbar, A.D., 2011. Molybdenum isotope constraints on the extent of late Paleoproterozoic ocean euxinia. Earth Planet. Sci. Lett. 307, 450–460.
Kendall, B., Komiya, T., Lyons, T.W., Bates, S.M., Gordon, G.W., Romaniello, S.J., Jiang, G., Creaser, R.A., Xiao, S., McFadden, K., Sawaki, Y., Tahata, M., Shu, D., Han, J., Li, Y., Chu, X., Anbar, A.D., 2015. Uranium and molybdenum isotope evidence for an episode of widespread ocean oxygenation during the late Ediacaran period. Geochim. Cosmochim. Acta 156, 173–193.
Kendall, B., Dahl, T.W., Anbar, A.D., 2017. The stable isotope geochemistry of molybdenum. Rev. Mineral. Geochem. 82, 683–732.
Kerl, C.F., Lohmayer, R., Bura-Nakic, E., Vance, D., Planer-Friedrich, B., 2017. Experimental confirmation of isotope fractionation in thiomolybdates using ion chromatographic separation and detection by multicollector ICPMS. Anal. Chem. 89, 3123–3129.
Lyons, T.W., Anbar, A.D., Severmann, S., Scott, C., Gill, B.C., 2009. Tracking euxinia in the ancient ocean: a multiproxy perspective and proterozoic case study. Annu. Rev. Earth Planet. Sci. 37, 507–534.
Manske, A.K., Glaeser, J., Kuypers, M.M., Overmann, J., 2005. Physiology and phylogeny of green sulfur bacteria forming a monospecific phototrophic assemblage at a depth of 100 meters in the Black Sea. Appl. Environ. Microbiol. 71, 8049–8060.
Musat, N., Halm, H., Winterholler, B., Hoppe, P., Peduzzi, S., Hillion, F., Horreard, F., Amann, R., Jorgensen, B.B., Kuypers, M.M., 2008. A single-cell view on the ecophysiology of anaerobic phototrophic bacteria. Proc. Natl. Acad. Sci. U. S. A. 105, 17861–17866.

Nägler, T.F., Neubert, N., Böttcher, M.E., Dellwig, O., Schnetger, B., 2011. Molybdenum isotope fractionation in pelagic euxinia: evidence from the modern Black and Baltic Seas. Chem. Geol. 289, 1–11.
Nägler, T.F., Anbar, A.D., Archer, C., Goldberg, T., Gordon, G.W., Greber, N.D., Siebert, C., Sohrin, Y., Vance, D., 2013. Proposal for an international molybdenum isotope measurement standard and data representation. Geostand. Geoanal. Res. 149–151.
Neubert, N., Nägler, T.F., Böttcher, M.E., 2008. Sulfidity controls molybdenum isotope fractionation into euxinic sediments: evidence from the modern Black Sea. Geology 36, 775–778.
Noordmann, J., Weyer, S., Montoya-Pino, C., Dellwig, O., Neubert, N., Eckert, S., Paetzel, M., Böttcher, M.E., 2015. Uranium and molybdenum isotope systematics in modern euxinic basins: case studies from the central Baltic Sea and the Kyllaren fjord (Norway). Chem. Geol. 396, 182–195.
Pearce, C.R., Cohen, A.S., Coe, A.L., Burton, K.W., 2008. Molybdenum isotope evidence for global ocean anoxia coupled with perturbations to the carbon cycle during the Early Jurassic. Geology 36, 231–234.
Reitz, A., Wille, M., Nagler, T., Delange, G., 2007. Atypical Mo isotope signatures in eastern Mediterranean sediments. Chem. Geol. 245, 1–8.
Scholz, F., McManus, J., Sommer, S., 2013. The manganese and iron shuttle in a modern euxinic basin and implications for molybdenum cycling at euxinic ocean margins. Chem. Geol. 355, 56–68.
Scott, C., Lyons, T.W., 2012. Contrasting molybdenum cycling and isotopic properties in euxinic versus non-euxinic sediments and sedimentary rocks: refining the paleoproxies. Chem. Geol. 324–325, 19–27.
Siebert, C., Nägler, T.F., von Blanckenburg, F., Kramers, J.D., 2003. Molybdenum isotope records as a potential new proxy for paleoceanography. Earth Planet. Sci. Lett. 211, 159–171.
Taylor, S.R., McLennan, S.M., 1995. The geochemical evolution of the continental crust. Rev. Geophys. 33, 241–265.
Tonolla, M., Peduzzi, R., Hahn, D., 2005. Long-term population dynamics of phototrophic sulfur bacteria in the chemocline of Lake Cadagno, Switzerland. Appl. Environ. Microbiol. 71, 3544–3550.
Tossell, J.A., 2005. Calculating the partitioning of the isotopes of Mo between oxidic and sulfidic species in aqueous solution. Geochim. Cosmochim. Acta 69, 2981–2993.
Tribovillard, N., Algeo, T.J., Baudin, F., Riboulleau, A., 2012. Analysis of marine environmental conditions based onmolybdenum–uranium covariation—Applications to Mesozoic paleoceanography. Chem. Geol. 324–325, 46–58.
Vorlicek, T.P., Helz, G.R., 2002. Catalysis by mineral surfaces: implications for Mo geochemistry in anoxic environments. Geochim. Cosmochim. Acta 66, 3679–3692.
Vorlicek, T.P., Kahn, M.D., Kasuya, Y., Helz, G.R., 2004. Capture of molybdenum in pyrite-forming sediments: role of ligand-induced reduction by polysulfides. Geochim. Cosmochim. Acta 68, 547–556.
Wagner, M., Chappaz, A., Lyons, T.W., 2017. Molybdenum speciation and burial pathway in weakly sulfidic environments: Insights from XAFS. Geochim. Cosmochim. Acta 206, 18–29.
Wichard, T., Mishra, B., Myneni, S.C.B., Bellenger, J.-P., Kraepiel, A.M.L., 2009. Storage and bioavailability of molybdenum in soils increased by organic matter complexation. Nat. Geosci. 2, 625–629.
Wille, M., Kramers, J.D., Nägler, T.F., Beukes, N.J., Schröder, S., Meisel, T., Lacassie, J.P., Voegelin, A.R., 2007. Evidence for a gradual rise of oxygen between 2.6 and 2.5 Ga from Mo isotopes and Re-PGE signatures in shales. Geochim. Cosmochim. Acta 71, 2417–2435.
Wirth, S.B., Gilli, A., Niemann, H., Dahl, T.W., Ravasi, D., Sax, N., Hamann, Y., Peduzzi, R., Peduzzi, S., Tonolla, M., Lehmann, M.F., Anselmetti, F.S., 2013. Combining sedimentological, trace metal (Mn, Mo) and molecular evidence for reconstructing past water-column redox conditions: the example of meromictic Lake Cadagno (Swiss Alps). Geochim. Cosmochim. Acta 120, 220–238.